NUKLEONIKA 2013;58(3):359–363

ORIGINAL PAPER

EPR study of ZnO:Co thin films grown by the PLD method

Bogumił Cieniek,
Ireneusz Stefaniuk,
Ihor Virt

Abstract. We have studied magnetic properties of zinc-oxide composite doped with a relatively high concentration (4%) of Co ions. Samples were obtained by the pulsed laser deposition (PLD) method with different parameters of the laser ablation. For various samples, the power of laser was changed as well as the temperature of sample heating. Electron paramagnetic resonance (EPR) measurements were carried out and temperature dependence of the EPR spectra was obtained. Analysis of the temperature dependences of the integral intensity of EPR spectra was carried out using the Curie-Weiss law. Fitting yields the following values $\theta_{CW} = 150$ K and $C = 1.67^{10}$, where C is the Curie constant, and θ_{CW} is the paramagnetic Curie temperature.

Key words: electron paramagnetic resonance (EPR) • diluted magnetic semiconductor (DMS) • ZnO:Co • Curie temperature

B. Cieniek✉, I. Stefaniuk, I. Virt
Institute of Physics,
University of Rzeszów,
16a Rejtana Str., 35-310 Rzeszów, Poland,
Tel.: +48 17 872 1094, Fax: +48 17 872 1283,
E-mail: cieniek@if.univ.rzeszow.pl

Received: 17 August 2012
Accepted: 4 January 2013

Introduction

Huge interest in ferromagnetic semiconductors with a wide energy gap is associated with the capabilities of their various applications such as in spintronics and the so-called semi-transparent electronics [4]. Due to the rare physical properties (the energy gap of about 3.4 eV at room temperature, the exciton binding energy of about 60 meV), ZnO is used for devices based on semiconductor structures [30, 31], such as varistors [34] or sensors [32]. Relatively simple production technology of ZnO crystals gives us the hope for lower cost of production equipment based on ZnO in comparison to the popular GaN. In addition, because of the ferromagnetic properties, this oxide can be used as a diluted magnetic semiconductor (DMS).

DMS are of interest for studing their unique spintronics properties with possible technological applications [8, 15], such as spin-spin exchange interaction between the localized magnetic moments and the band electrons [6]. This property of DMS has potential applications in the spin-dependent semiconductor electronics [2].

Some subsequent theoretical approach using density functional theory (DFT) [20, 21] and experimental [16, 26] works show that the n-type Co-doped ZnO also possesses room temperature ferromagnetism.

Some authors have reported ferromagnetism in ZnO doped with transition metal systems at the Curie temperatures T_C ranging from 30 to 550 K [3, 11, 14, 22,

23, 26, 29] while others have found antiferromagnetic, spin glass, or paramagnetic behaviour [1, 12, 28].

The existence of ferromagnetic ordering in (Zn,Co)O has been theoretically proposed to be attributed to the double exchange interaction [20, 21] or to the RKKY interaction between Co ions [10]. Later calculation showed that the ground state of Co-doped ZnO is the spin glass without doping due to the short range interactions between transition metal atoms [13].

According to the theory of Dietl *et al*. [5], the p-d interactions are the reason for the long-range magnetic coupling. However, the investigated magnetic ZnO samples are either n-type conducting or insulating. The observed weak ferromagnetism in implanted ZnO, containing ferromagnetic nanocrystals and in PLD grown ZnO with diluted magnetic ions, is due to the ferromagnetic nanocrystals and the acceptor-like defects [33], respectively. For the diluted ZnCoO, it would be interesting to check if there is an interaction between the free electrons and d-electrons in the Co ions, and if this s-d interaction results in ferromagnetic coupling.

We report here the magnetic properties of zinc-oxide composite (ZnO) doped with Co. Electron paramagnetic resonance (EPR) spectra have been measured and analyzed to extract information on the characteristics of the incorporation of the ions in the lattice.

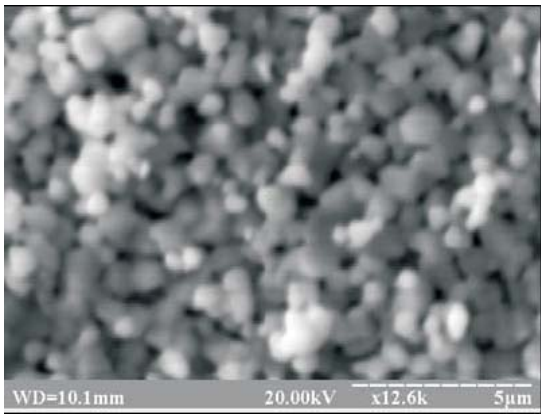

Fig. 1. Characteristics of the sample ZnO:Co, TEM image.

Experimental

Samples of zinc-oxide doped with cobalt were obtained by the pulsed laser deposition (PLD) method with different parameters of the laser ablation. For various samples, the power of laser was changed (from 6 up to 600 impulses), as well as temperature of sample heating. Only some of the samples were heated at 573 K. The concentration of Co was found by the proportions of ZnO and CoO, $(ZnO)_{96}$ and $(CoO)_4$ to make a target of the PLD method (described in detail in work [25]). EPR measurements were performed with a modified X-band EPR spectrometer [24]. The temperature of the samples was controlled in the range of 100–370 K using a BRUKER liquid N gas flow cryostat.

Results and discussion

Transmission electron microscopy (TEM) images of the investigated samples of ZnO:Co are presented in Fig. 1. We included TEM image to show the morphology of the sample and present the material structure. The sample of ZnO:Co have porous structure with different graininess. The thickness of the layer, measured by scanning electron microscopy (SEM) was about 500 nm.

EPR spectra as a function of temperature for the annealed and non-annealed sample are shown in Figs. 2 and 3, respectively.

EPR spectra of annealed and non-annealed layers are similar with one difference, i.e. in the EPR spectrum of non-annealed layer appears an additional line with a value of $g = 1.96$ which can be associated with defects. Recently, it was concluded that the g-factor of

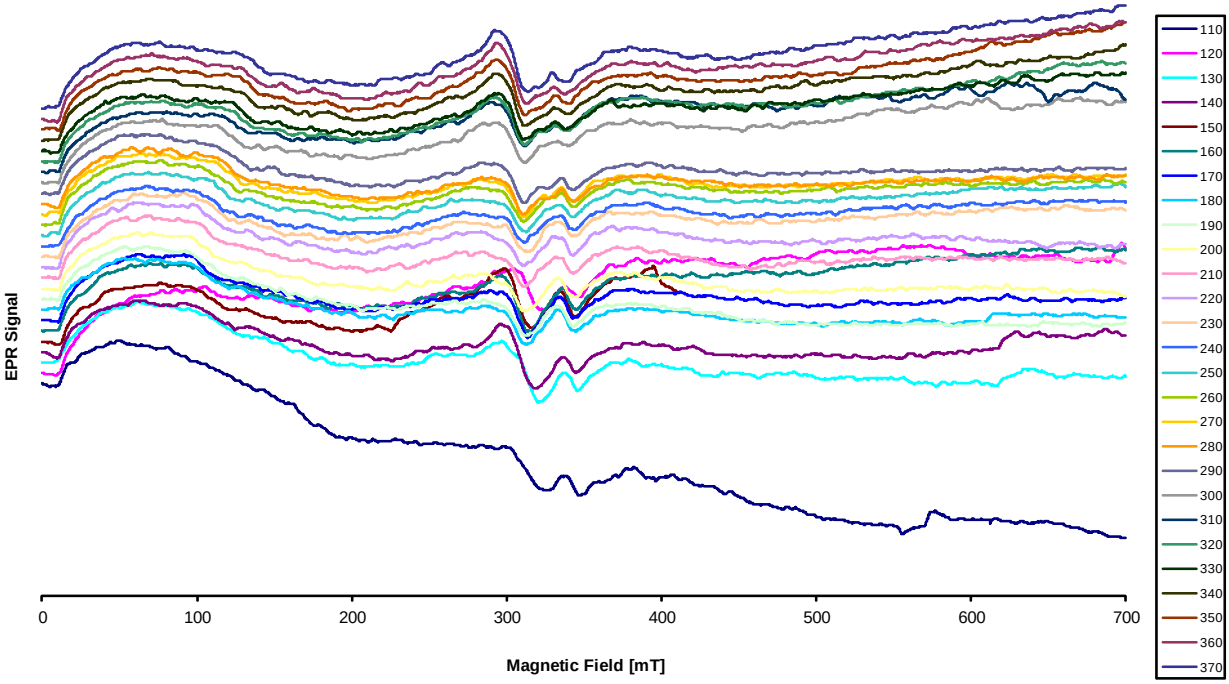

Fig. 2. EPR spectra of ZnCoO non-annealed sample (obtained at 600 pulses) at various temperatures.

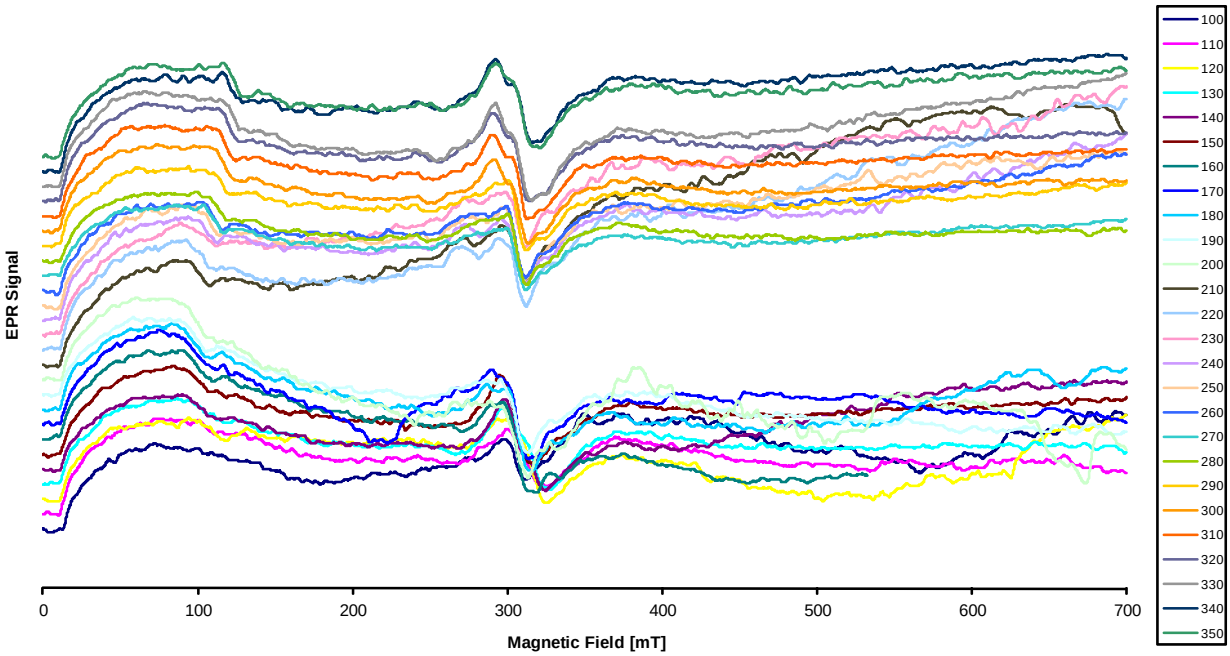

Fig. 3. EPR spectra of ZnCoO annealed sample (obtained at 600 pulses) at various temperatures.

1.96 is related to the oxygen vacancy, which was found by means of optically detected magnetic resonance [17, 27]. For samples obtained with a smaller number of pulses, the spectrum EPR are very similar, differing only in intensity. This is closely related to the thickness of the obtained layer, because for 600 pulses the greatest thickness was obtained, and, therefore, the signal is most intense. EPR spectra were analyzed for the layer of annealed and non-annealed ZnCoO.

The effective spectroscopic *g*-factor and the peak-to-peak line width (*H*pp) of the resonance line were determined. Since the broad EPR line is asymmetric, the accuracy of parameters measured directly from the experimental spectrum is rather limited. Therefore, additionally the experimental line was fitted using the Lorenzian type curve, since such curves describe satisfactorily experimental EPR lines of DMS with manganium in high temperature range (see [18], and references therein). In this way we determined parameters for EPR lines such as the peak-to-peak line width (*H*pp), the intensity (*I*) as well as the resonance field (*H*r) (Table 1). Based on these data, we obtained the temperature dependencies of gyromagnetic factor $g(T)$ $Hr(T)$, and integral intensity as presented in Figs. 4 and 5, respectively. At fitting the Lorenz type curve, the lower field part of the EPR line was included because of its regular nature.

Table 1. Numerical values of *g*-factor, *H*r, *H*pp and *I*

Temperature (K)	*g*-factor	*H*r (mT)	*H*pp	*I*
340	2.1950	302.06	18.46	246
330	2.2004	301.33	19.59	224
320	2.1968	301.82	20.32	225
310	2.2022	301.08	20.76	210
300	2.2055	300.63	23.88	197
290	2.2243	298.09	25.89	188
280	2.2294	297.41	26.75	177
270	2.2296	297.39	27.73	178
260	2.2511	294.54	31.96	165
250	2.2462	295.18	34.95	153
240	2.2538	294.18	34.56	142
230	2.2530	294.29	34.69	140
220	2.2609	293.26	34.18	160
210	2.2371	296.39	30.15	168
200	2.2328	296.96	27.81	177
190	2.2155	299.27	27.58	193
180	2.2163	299.16	26.66	200
170	2.1981	301.64	23.93	223
160	2.1647	306.29	19.23	265
150	2.1557	307.57	17.86	282
140	2.1590	307.10	22.39	304
130	2.1479	308.69	23.67	255
120	2.1074	314.62	21.53	208
110	2.1276	311.63	28.88	208

We used the Curie-Weiss law to analyze the temperature dependences of the integral intensity, which is directly proportional to the magnetic susceptibility χ. A linear increase of χ^{-1} (T) at higher temperatures can be fitted to the Curie-Weiss law [7, 9].

$$(1) \qquad (\chi(T) - \chi_0)^{-1} = (T - \theta_{CW}) / C$$

where C is the Curie constant, θ_{CW} is the paramagnetic Curie temperature, and χ_0 is a temperature independent

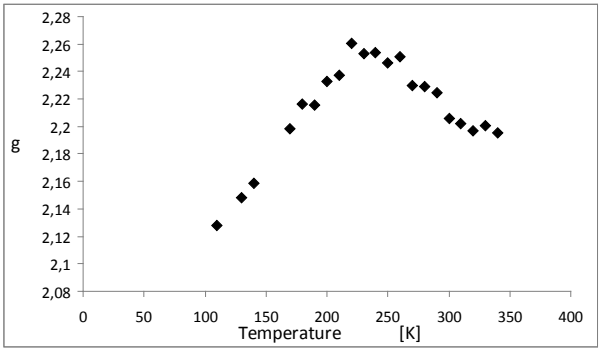

Fig. 4. Temperature dependence of *g*-factor for an annealed layer.

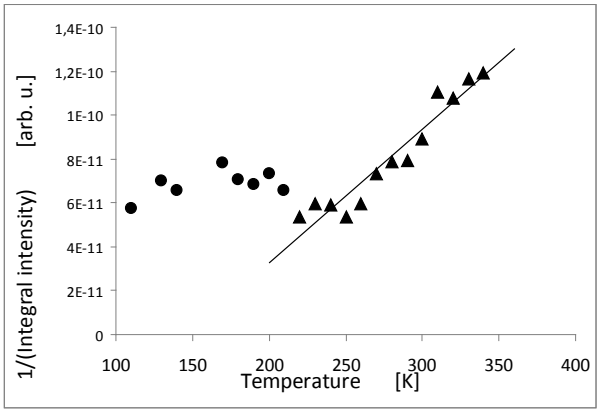

Fig. 5. Temperature dependence of the 1/(integral intensity) for an annealed layer.

term to account for the diamagnetic host and any Pauli paramagnetism contribution. Figure 5 displays the temperature dependence of the quantity $(\chi(T) - \chi_0)^{-1}$. The line is a linear extrapolation illustrating the ferromagnetic (positive) Curie-Weiss temperature. Fitting yields the following values $\theta_{CW} = 150$ K and $C = 1.67$[10].

Conclusions

For annealed and non-annealed layers, the observed characteristic temperature around 220 K in which all EPR line parameters such as: peak-to-peak line width (Hpp), the intensity (I) as well as the gyromagnetic factor $g(T)$ are changed.

In summary, we have reported the X-band EPR studies of ZnO:Co. From the EPR lines we have determined the parameters: peak-to-peak line width (Hpp), intensity (I) as well as the resonance field (Hr). The results of temperature dependence of EPR spectra for the sample ZnO:Co and linear extrapolations to the Curie-Weiss law indicate the ferromagnetic interaction between the Co ions characterized by the Curie temperature 150 K.

By analyzing the EPR linewidth behaviour, the same as in [19], we claim that a combined effect of the exchange and dipolar broadening plays an important role in the mechanism of linewidth formation in this material.

References

1. Ankiewicz AO, Gehlhoff W, Kaidashev EM *et al*. (2007) Electron paramagnetic resonance in transition metal--doped ZnO nanowires. J Appl Phys 101:024324
2. Awshalom DD, Loss D, Samarth N (eds) (2002) Semiconductors spintronics and quantum computation. Springer, New York
3. Cho YM, Choo WK, Kim H, Kim D, Ihm YE (2002) Effects of rapid thermal annealing on the ferromagnetic properties of sputtered $Zn_{1-x}(Co_{0.5}Fe_{0.5})_xO$ thin films. Appl Phys Lett 80:3358–3360
4. Dietl T (2007) Origin of ferromagnetic response in diluted magnetic semiconductors and oxides. J Phys: Condens Matter 19:165204
5. Dietl T, Ohno H, Matsukura F, Cibert J, Ferrand D (2000) Zener model description of ferromagnetism in zinc-blende magnetic semiconductors. Science 287:1019–1022
6. Dobrowolski W, Kossut J, Story T (2003) II-VI and IV-VI diluted magnetic semiconductors – new bulk materials and low dimensional quantum structures. In: Buschow KHJ (ed) Handbook of magnetic materials. Vol. 15. Elsevier, The Netherlands, pp 289–378
7. Dyck JS, Drašar Č, Lošťák P, Uher C (2005) Low-temperature ferromagnetic properties of the diluted magnetic semiconductor $Sb_{2-x}Cr_xTe_3$. Phys Rev B 71:115214
8. Furdyna JK (1988) Diluted magnetic semiconductors. J Appl Phys 64:R29 (36 pp)
9. Huber DL, Alejandro G, Caneiro A *et al*. (1999) EPR linewidths in $La_{12x}Ca_xMnO_3$: $0 < x < 1$. Phys Rev B 60:12155–12161
10. Jalbout AF, Chen H, Whittenburg SL (2002) Monte Carlo simulation on the indirect exchange interactions of Co-doped ZnO film. Appl Phys Lett 81:2217–2219
11. Jung SW, An S-J, Yi G-C, Jung CU, Lee S-I, Cho S (2002) Ferromagnetic properties of $Zn_{1-x}Mn_xO$ epitaxial thin films. Appl Phys Lett 80:4561–4563
12. Kim JH, Kim H, Ihm YE, Choo WK (2002) Magnetic properties of epitaxially grown semiconducting $Zn_{1-x}Co_xO$ thin films by pulsed laser deposition. J Appl Phys 92:6066–6071
13. Lee E-C, Chang KJ (2004) Ferromagnetic versus antiferromagnetic interaction in Co-doped ZnO. Phys Rev B 69:085205
14. Lee H-J, Jeong S-Y, Cho CR, Park CH (2002) Study of diluted magnetic semiconductor: Co-doped ZnO. Appl Phys Lett 81:4020–4022
15. Ohno H (1998) Making nonmagnetic semiconductors ferromagnetic. Science 281:951–956
16. Prellier W, Fouchet A, Mercey B, Simon Ch, Raveau B (2003) Laser ablation of Co:ZnO films deposited from Zn and Co metal targets on (0001) Al_2O_3 substrates. Appl Phys Lett 82:3490–3492
17. Romanov NG, Tolmachev DO, Badalyan AG, Babunts RA, Baranov PG, Dyakonov VV (2009) Spin-dependent recombination of defects in bulk ZnO crystals and ZnO nanocrystals as studied by optically detected magnetic resonance. Physica B 404:4783–4786
18. Samarth N, Furdyna JK (1988) Electron paramagnetic resonance in $Cd_{1-x}Mn_xS$, $Cd_{1-x}Mn_xSe$, and $Cd_{1-x}Mn_xTe$. Phys Rev B 37:9227–9239
19. Sati P, Pashchenko, Stepanov A (2007) Exchange broadening of EPR line in ZnO:Co. Fizika Nizkikh Temperatur 33;11:1222–1226
20. Sato K, Katayama-Yoshida H (2000) Material design for transparent ferromagnets with ZnO-based magnetic semiconductors. Jpn J Appl Phys 39:L555–L558
21. Sato K, Katayama-Yoshida H (2001) Stabilization of ferromagnetic states by electron doping in Fe-, Co- or Ni-doped ZnO. Jpn J Appl Phys 40:L334–L336
22. Schwartz DA, Norberg NS, Nguyen QP, Parker JM, Gamelin DR (2003) Magnetic quantum dots: synthesis, spectroscopy, and magnetism of Co^{2+}- and Ni^{2+}-doped ZnO nanocrystals. J Am Chem Soc 125:13205–13218
23. Sharma P, Gupta A, Rao KV *et al*. (2003) Ferromagnetism above room temperature in bulk and transparent thin films of Mn-doped ZnO. Nat Mater 2:673–677
24. Stefaniuk I, Cieniek B (2012) A multifunctional computer system for use with an EPR spectrometer. Elektronika 53;2:96–99
25. Stefaniuk I, Cieniek B, Virt I (2010) Magnetic properties of zinc-oxide composite doped with transition metal ions (Mn, Co, Cr). Curr Top Biophys 33;Suppl A:221–226
26. Ueda K, Tabata H, Kawai T (2001) Magnetic and electric properties of transition-metal-doped ZnO films. Appl Phys Lett 79:988–900
27. Vlasenko LS, Watkins GD (2005) Optical detection of electron paramagnetic resonance in room-temperature electron-irradiated ZnO. Phys Rev B 71:125210

28. Volbers N, Zhou H, Knies C *et al*. (2007) Synthesis and characterization of ZnO:Co^{2+} nanoparticles. Appl Phys A: Mater Sci Process 88:153–155
29. Wakano T, Fujimura N, Morinaga Y, Abe N, Ashida A, Ito T (2001) Magnetic and magneto-transport properties of ZnO:Ni films. Physica E 10:260–264
30. Weng J, Hang Y, Han G *et al*. (2005) Electrochemical deposition and characterization of wide band semiconductor ZnO thin film. Thin Solid Films 478:25–29
31. Wilkinson J, Ucer KB, Wiliams RT (2004) Picosecond excitonic luminescence in ZnO and other wide-gap semiconductors. Radiat Meas 38:501–505
32. Xu J, Pan Q, Shun Y, Tian Z (2000) Grain size control and gas sensing properties of ZnO gas sensor. Sens Actuators B 66:277–279
33. Xu Q, Schmidt H, Zhou S *et al*. (2008) Room temperature ferromagnetism in ZnO films due to defects. Appl Phys Lett 92:082508
34. Ya KX, Yin H, De TM, Jing TM (1998) Analysis of ZnO varistors prepared from nanosize ZnO precursors. Mater Res Bull 33:1703–1708